# CHAPTER 8

## EFFECT OF IODINE CONCENTRATIONS, TEMPERATURE AND LIGHT INTENSITY ON THE PERFORMANCE OF PEC SOLAR CELLS USING $MoSe_xTe_{2-x}$ SINGLE CRYSTALS

CONTENTS PAGES

## 8.1 Introduction

There have been several discussions in recent years on photoelectrochemical (PEC) methods of solar energy conversion. An important factor affecting the conversion efficiency is the electrolyte. The detailed studies have been carriedout out by various workers[1-13] on the photoelectrochemical behaviour in contact with different aqueous and non-aqueous redox electrolytes. Their results have indicatee that iodine/iodide, $I_2/I^-$ system to be optimal redox couple for the best performance and stability. Since the light conversion efficiency of the cell based on $I_2$ / $I^-$ depends upon iodine contact of the redox couple, the iodine concentration has been optimised in the present work for better conversion efficiencies of $MoSe_2Te_{2-x}$ photoelectrodes.

A key element of PEC devices is the semiconductor electrolyte interface. The degree of effectiveness of minority carrier charge transfer across their interface will have direct bearing on the ultimate energy conversion efficiency of the system.

The strategy of enbancing this charge exchange by elec ting the temperature has the added advnatage of utilizing the near IR region of solar spectrum, which otherwise would be wasted. Temperature also has beneficial effects on the optical properties of the semiconductor. An effort has therefore been made to critically evaluate the effect of temperature on the photovoltaic performance of $MoSe_2Te_{2-x}$ photoelectrodes.

Further, since the efficiency and behaviour of most photoelectrodes in photoelectrochemical solar cells depend on the characteristics of the incident light, author has described such studies on PEC cells based on $MoSe_xTe_{2-x}$ in this chapter.

## 8.2 Results and Discussion

### 8.2.1 Iodine Concentration Effect

The grown single crystals of $MoSe_xTe_{2-x}$ as photoelectrodes and platinum grid as counter electrode have been used for fabrication of PEC cells. The photoelectrochemical glass cell (Fig. 8.1) has been so designed that the electrolyte can be changed without

disturbing the electrode position. Electrolytes of different concentrations of iodine are prepared by addition of 2 M NaI and 0.5 M $Na_2SO_4$ in double distilled water. All chemicals are of A.R. grade. The effect of iodine concentration on the efficiency ($\eta$ %) for $MoSe_2Te_{2-x}$, $0 \leq x \leq 2$ is shown in Fig. 8.2. The decrease in efficiency at higher concentrations of iodine is due to absorption of light in electrolyte which results into lower short-circuit currents. The decrease in efficiencies can also bee attributed to the presence of large amounts of elemental iodine which can interact with the surface and generate surface states which can trap charges of either sign. This causes large charges of potential drop in Helmoltz double layer as well as shifts in the energy position on band edges. The amount of iodine adsorption, which affects the band bending in the semiconductor can also be considered as a factor affecting efficiency[9].

### 8.2.2 Temperature Effect

The photoelectrochemical solar cell assembly was set up by using $MoSe_xTe_{2-x}$ photoelectrodes

and platinum grid as counter electrode. Iodine/Iodide ($I_2$ / $I^-$) electrolyte was prepared by mixing AR grade 0.025 M $I_2$, 5.0 M NaI, 0.5 M $Na_2SO_4$ in doubly distilled water. The temperature of electrolyte was measured by a mercury thermometer. Photocurrent-voltage measurements were made at different temperatures, keeping the intensity of illumination constant. An incandescent lamp was used as a source of light. During the heating, electrolyte in the PEC cell was continuously stirred with a magnetic stirrer to maintain an uniform temperature.

The effect of temperature on the short circuit current ($I_{SC}$) and open circuit voltages, at different temperatures is illustrated in Figure 8.3. The open circuit voltages are found to decrease with increase in the temperature. This decreasing trend of $V_{OC}$ is in confirmation with the observations of Kazacoss et al[14] and Agarwal et al[15] for $MoSe_2$ and $MoTe_2$. This decrease in open circuit voltage $V_{OC}$ at higher temperature can be explained by applying Schottky barrier model through the equation

$$V_{OC} = \frac{nKT}{q} \ln \left( \frac{I_{ph}}{I_o} \right)$$

$$I_O = A^* T^2 \exp \left( - \phi_b / KT \right)$$

Here $A^*$ is Richardson constant, and $\phi_b$ is barrier height. Therefore, according to Schottky barrier model the open circuit voltage $V_{OC}$, depends upon $I_o$, the reverse saturation current density, which in turn depends upon the temperature.

The initial increase in short circuit current $I_{SC}$ is attributed to the increase in absorption co-efficient of the semiconductor[16]. According to K. Rajeshwar et al[17] the increase in short circuit current $I_{SC}$ has its origin both on temperature induced changes in the optical and electrical properties of semiconductor and corresponding variations in the potential and charge distribution across the semiconductor-electrolyte interface. It is observed by Agarwal et al[18] that

1. The wavelength response shifts towards red

with increasing temperature because of band gap narrowing.

2. The diffusion length of photogenerated carriers increases with increasing temperature, and

3. The absorption coefficient at longer wavelength increases with increasing temperature because of band gap narrowing.

All this jointly causes increase in $I_{SC}$ with increasing temperature.

The increase in $I_{SC}$ is however, limited because of changes in series and shunt resistances of the cell with temperature. At higher temperature, shunt resistance decreases reducing the current in the cell. The bulk resistance of semiconductor also decreases with increasing temperature. The observed peak of current ($I_{ph}$) is a result of these two competing factors. At still higher temperatures shunt resistance of cell becomes smaller and the current decreases further. From fig. 8.3 the short circuit current, $I_{SC}$ for $MoSe_2$ is found

to decrease steadily with the increasing temperature. Similar trend in short circuit current is also observed by Kazacos et al[14] in case of $MoSe_2$. However, except $MoSe_2$ in the other compounds of the $MoSe_xTe_{2-x}$ series a peak in short circuit current is observed.

Figure 8.4 illustrates the variation of the efficiencies and fill factors of $MoSe_xTe_{2-x}$ PEC cells at different temperatures. The efficiencies and fill factors of the cells also pass through a peak at the temperature increases. Similar trends of efficiency and fill factor is also observed for $MoSe_2$ and $MoTe_2$ based PEC solar cells[14,15].

### 8.2.3 Effect of Illumination Intensity

The Schematic diagram of experimental set up for studying the effect of intensity of illumination is shown in Fig. 8.5. Fresh iodine/iodide electrolyte having the same concentration as used in the study of the effect of temperature, has been utilized in the present study. The incident light intensity was adjusted by changing the distance between PEC cell and light source.

The effect of illumination (light) intensity on the photocurrent photovoltage characteristics of $MoSe_xTe_{2-x}$ ($0 \leq x \leq 2$) is illustrated in Figs. 8.6(a), 8.6(b), 8.6(c), 8.6(d) and 8.6(e) respectively. Treating semiconductor-electrolyte interface as Schottky barrier, the current voltage characteristic is represented by the following expression,

$$J = J_{ph} - J_d = J_{ph} - J_o \left[\exp(qv/nkT) - 1\right] \tag{8.1}$$

Here J is net current density, $J_{ph}$ and $J_d$ are photocurrent and dark current densities. $J_o$ is the reverse saturation current density, V is voltage, n is "Junction Identify" factor and other terms have their usual significance. According to Rajeshwar et al[17] at equilibrium (open circuit condition), $J_{ph} = J_d$ and $V = V_{OC}$ so that rearrangement of equation (8.1) yields.

$$V_{OC} = \frac{nkT}{q} \ln \frac{J_{SC}}{J_o} \tag{8.2}$$

where $V_{OC}$ is the open circuit voltage, and

$J_{SC}$ is the short circuit current density.

If we further assume that $J_{SC} \propto J_C$ ( = incident light intensity) and $J_{SC} >> J_o$ , (Equation 8.2) reduces to following expression

$$V_{OC} \propto \frac{nkT}{q} \ln I_L$$

A plot of $V_{OC}$ against $\ln I_L$ yields a straight line from which n can be determined for particular device. An ideal device should have an n value of unity.

Figures 8.7(a), 8.7(b), 8.7(c), 8.7(d) and 8.7(e) show the plots of light intensity $I_L$, versus open circuit voltage $V_{OC}$, short circuit current $I_{SC}$ and logarithm of light intensity versus open circuit voltage for $MoSe_xTe_{2-x}$.

It is observed that the short circuit current varies linearly with light intensity, i.e.

$$I_{SC} = C\, I_L$$

where C is constant and

$I_L$ is the intensity of light.

However, all compounds indicate that the open circuit voltage ($V_{OC}$) is a linear function of logarithm of incident light intensity ($I_L$) (Figs. 8.7(a), 8.7(b), 8.7(c), 8.7(d) and 8.7(e) ).

The junction ideality factor for the $MoSe_xTe_{2-x}$ was determined from the plots of open circuit voltage $V_{OC}$ versus log $I_L$ from Figs. 8.7(a), 8.7(b), 8.7(c), 8.7(d) and 8.7(e) and compared with the reported values in Table 8.1. The lowest junction ideality factor 2.0 was for $MoSe_2$ samples. The high values of junction ideality factor indicate the characteristics of recombination process in space charge layer. Tunneling currents and interfacial layers can result in considerable higher values of n equal to or greater than 2[19].

The effect of light intensity on the light to electricity conversion efficiency ($\eta$) and fill factors of $MoSe_xTe_{2-x}$ are given in Fig. 8.8. The decrease in efficiency at higher light

Table 8.1

Junction ideality factor for $MoSe_xTe_{2-x}$

| Compound | Ideality factor calculated 'n' | Ideality factor reported |
|---|---|---|
| $MoSe_2$ | 2 | 2.8[18] |
| $MoSe_{1.5}Te_{0.5}$ | 3.2 | |
| MoSeTe | 4.0 | |
| $MoSe_{0.5}Te_{1.5}$ | 4.8 | |
| $MoTe_2$ | 3.2 | |

intensities was attributed to [20] loss of fill factor at higher light intensities.

## 8.3 Conclusion

1. The efficiency, fill factor, open circuit voltage and short circuit current of PEC cell is found to depend upon the electrolyte content concentration (iodine) and operating temperature of cell.

2. The open circuit voltages shows a decreasing trend in their values with the increase in temperature.

3. Peak in efficiency is found at about 308 K for all compounds ($MoSe_xTe_{2-x}$) except for $MoSe_{1.5}Te_{0.5}$.

4. The efficiency of light to electrical energy conversion for $MoTe_2$ and that of mixed compounds $MoSe_xTe_{2-x}$ is not as high as that for $MoSe_2$.

## REFERENCES


1. Tributsch, H. (1977)
   Ber. Bunsenges. Phys. Chem. 81, 361.

2. Kautck, W. and Gerischer, H. (1980)
   Ber. Bunsenges. Phys. Chem. 84, 645.

3. Kautek, W., Gerischer, H. and
   Tributsch, H. (1979)
   Ber. Bunsenges Phys. Chem. 83, 1000.

4. Agarwal, M. K., Patil, V. R. and
   Patel, P. D. (1982)
   J. Electrochem. Soc. India, 31, 3.

5. Tributsch, H., Gerischer, H.,
   Clemen, C. and Bucher, E. (1979)
   Ber. Bunsenges. Phys. Chem. 83, 655.

6. White, H. S., Abruna, H. D. and
   Bard, A. J. (1982)
   J. Electrochem. Soc. 129, 2, 265.

7. Tributsch, H. (1978)
   J. Electrochem. Soc. 125, 7, 1086.

8. Gobrecht, J., Tributsch, H. and Gerischer, H. (1978) J. Electrochem. Soc. 125, 12, 2086.

9. Kline, G., Kam, K. K., Canfield, D. and Parkinson, B. A. (1981) Sol. Energy. Mat. 4, 301.

10. Otto, H., Muller, N. and Gerischer, H. (1982) Electrochimica Acta 27, 8, 991.

11. Kubaik, C. P., Schneemeyer, L. F., and Wrighton, M. S. (1980) J. Am. Chem. Soc. 102, 6899.

12. Schneemeyer, L. F. and Wrighton, M. S. (1980) Appl. Phys. Lett. 36, 8, 701.

13. Philips, M. L. and Spitler, M. T. (1981) J. Electrochem. Soc. 128, 10, 2138.

14. Skyllas Kazaus, M., McCann, J. F. and Haneman, D. (1981) Sol. Energ. Mat. 4, 215.

15. Agarwal, M. K., Patel, P. D., Laxminarayana, D. and Talele L. T. (1984) (Proccedings of the conference on photo-voltaic materials and devices, 10-12 May 1984, held at National Physical Laboratory, New Delhi, India) P. 437.

16. Butler, M. A. (1977) J. Appl. Phys. 48, 1914.

17. Rajeshwar, K., Singh, P. and Thapar R. (1981) J. Electrochem. Soc. 128, 8, 1750.

18. Agarwal, A., Tiwary, V. K., Agarwal, S. K. and Jain, S. C. (1980) Solid State Electronics 23, 1021.

19. Rhoderick, E. H. (1978) "Metal-Semiconductor Contacts" P. G. Clarendon Press, Oxford.

20. Kline,G., Kam, K. K., Ziegler, R. and Parkinson B. A. (1982) Solar Energy Mat., 6, 337.

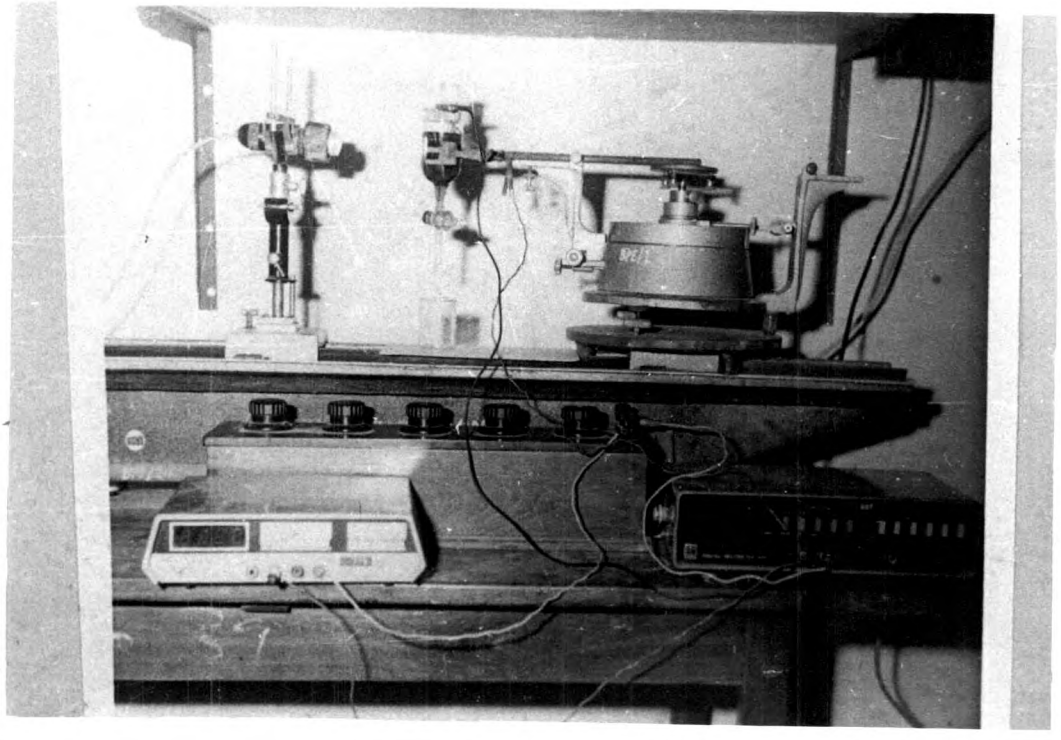

Fig. 8.1 Experimental set up of PECE cell for study of iodine concentrations.

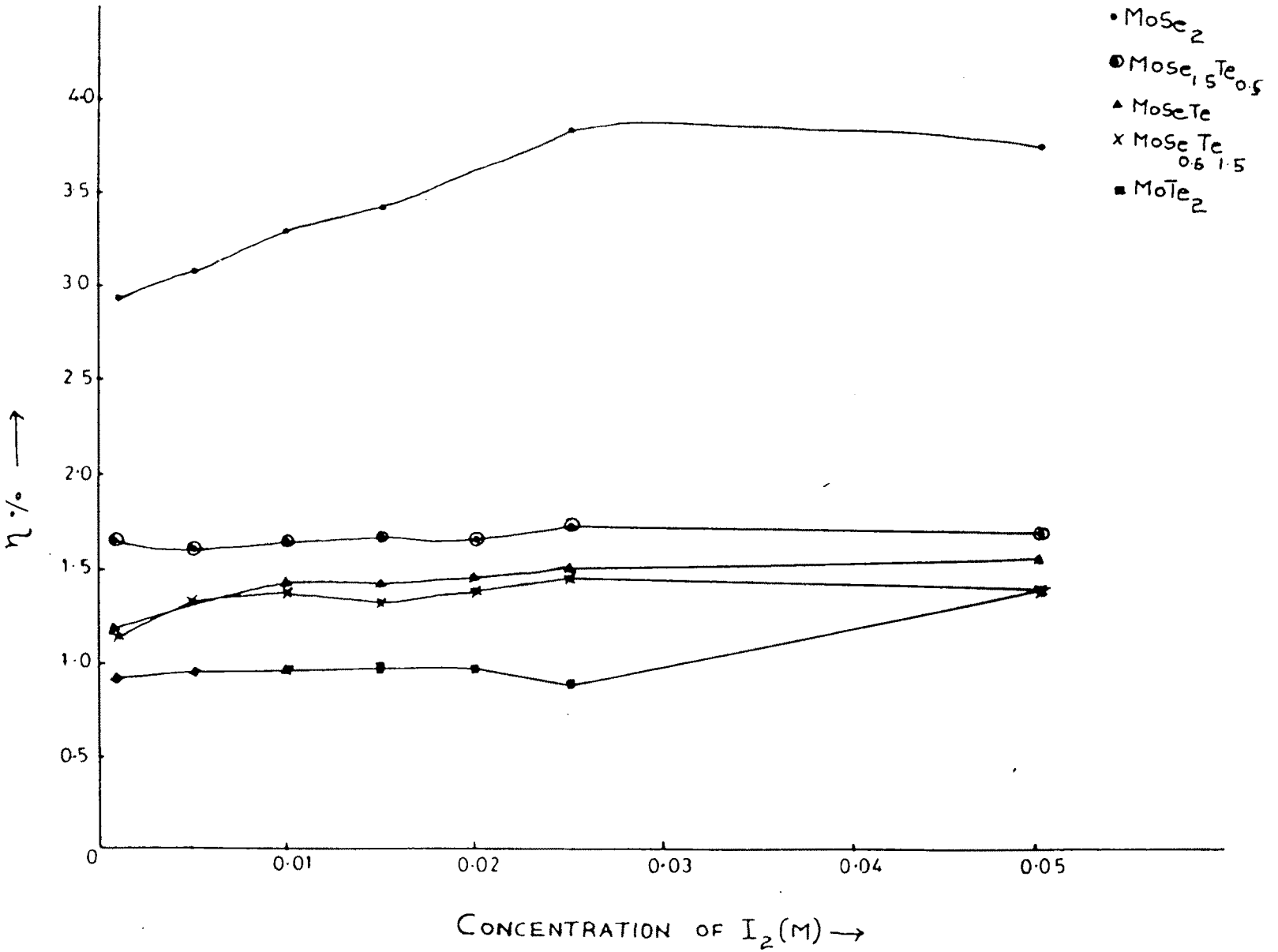


Fig. 8.2 Plots of efficiencies versus iodine concentrations $I_2$( M) for PEC cells with $MoSe_xTe_{2-x}$ photoelectodes.

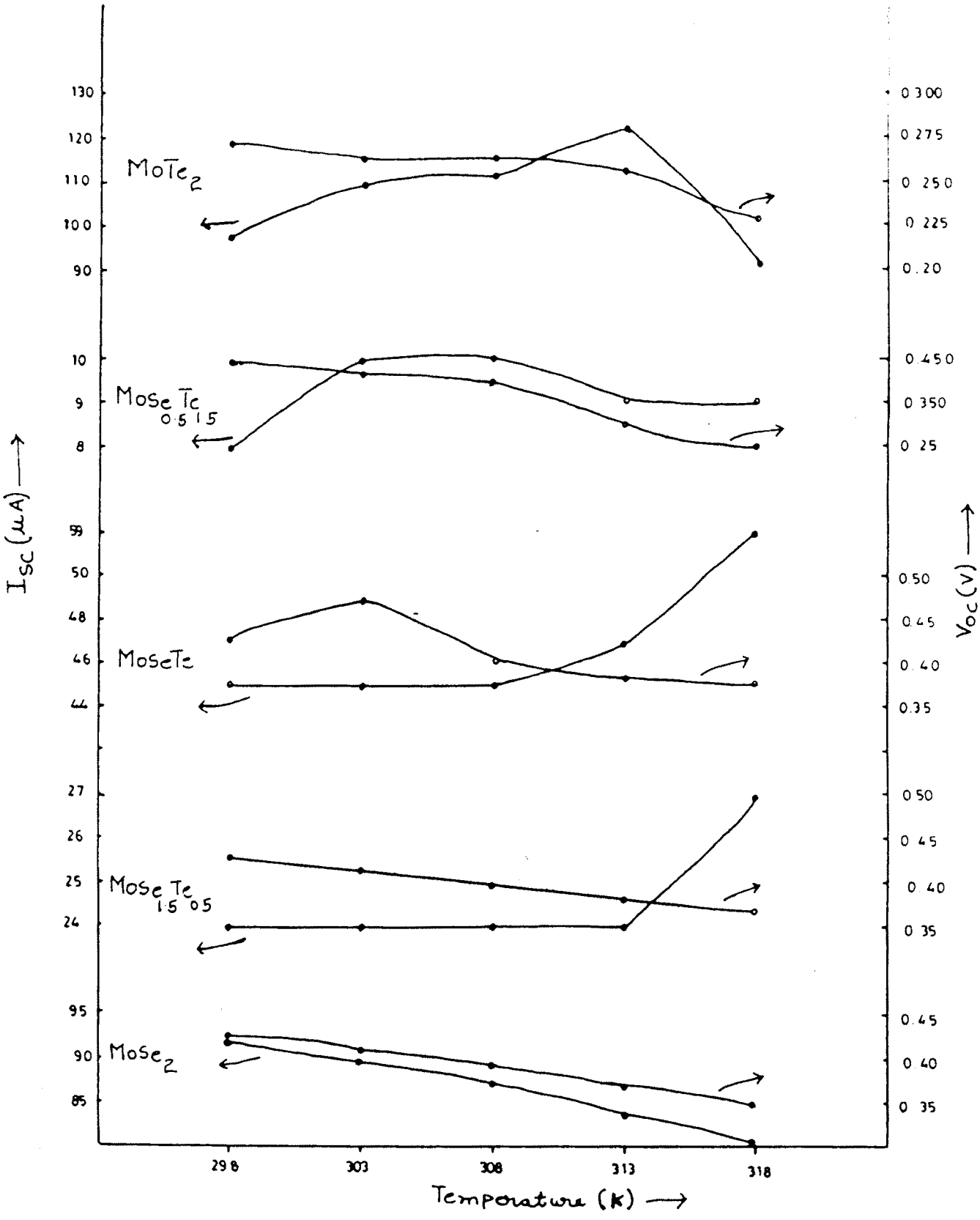


Fig. 8.3 Plots of variations of short-circuit current $I_{SC}$, and open circuit voltage $V_{OC}$ of $MoSe_xTe_{2-x}$ based PEC cells, with the temperature.

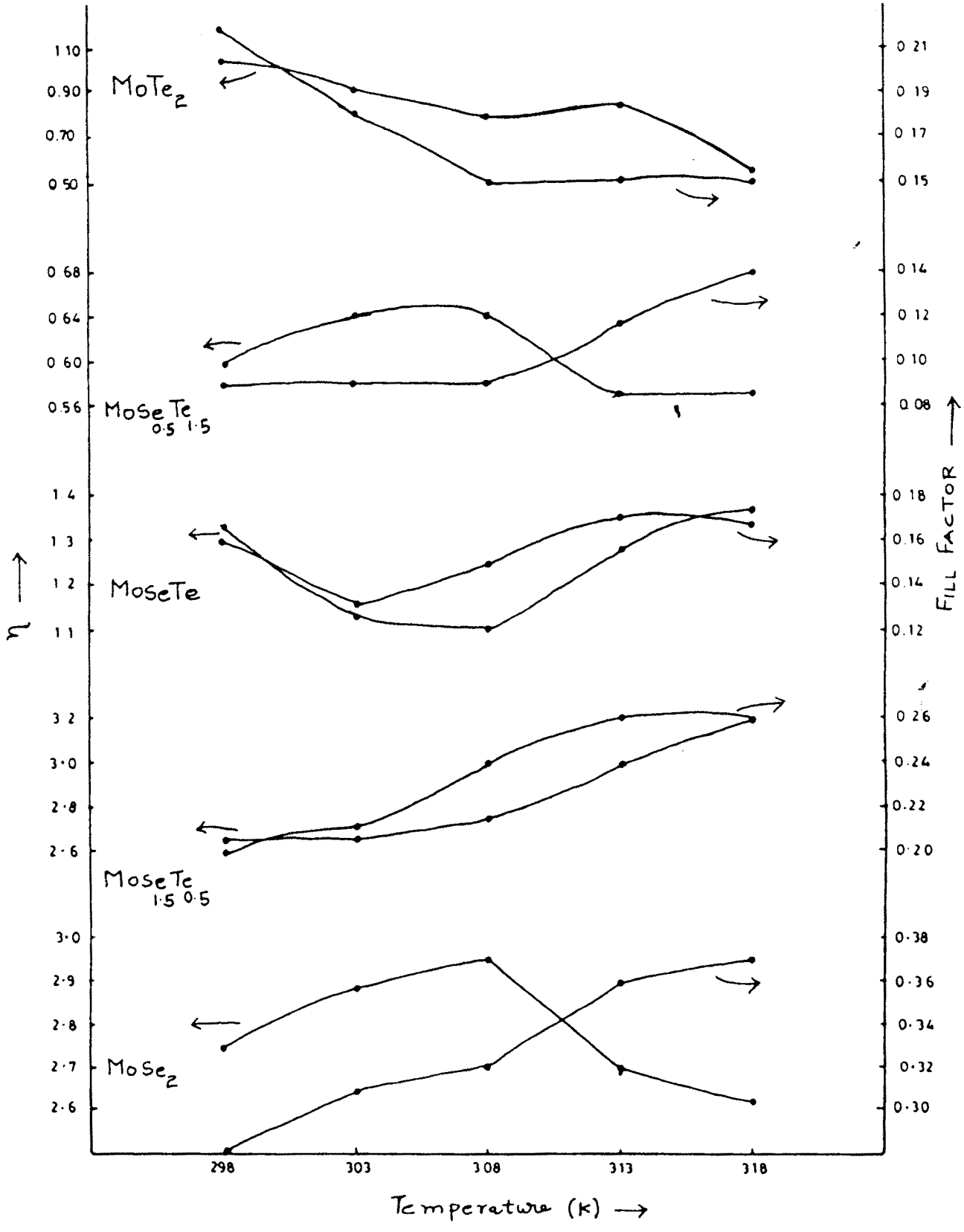


Fig. 8.4 Plots of variations of conversion efficiencies ($\eta$ %) and fill factors of $MoSe_xTe_{2-x}$ based PEC cells with the temperature.

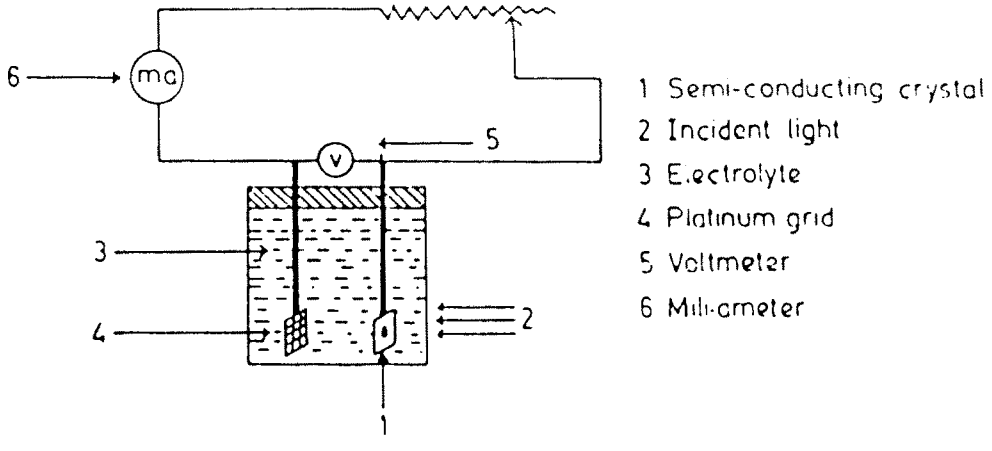


Fig. 8.5 PEC solar cell using $MoSe_xTe_{2-x}$ crystals as photoelectrodes and platinum grid as counter electrode.

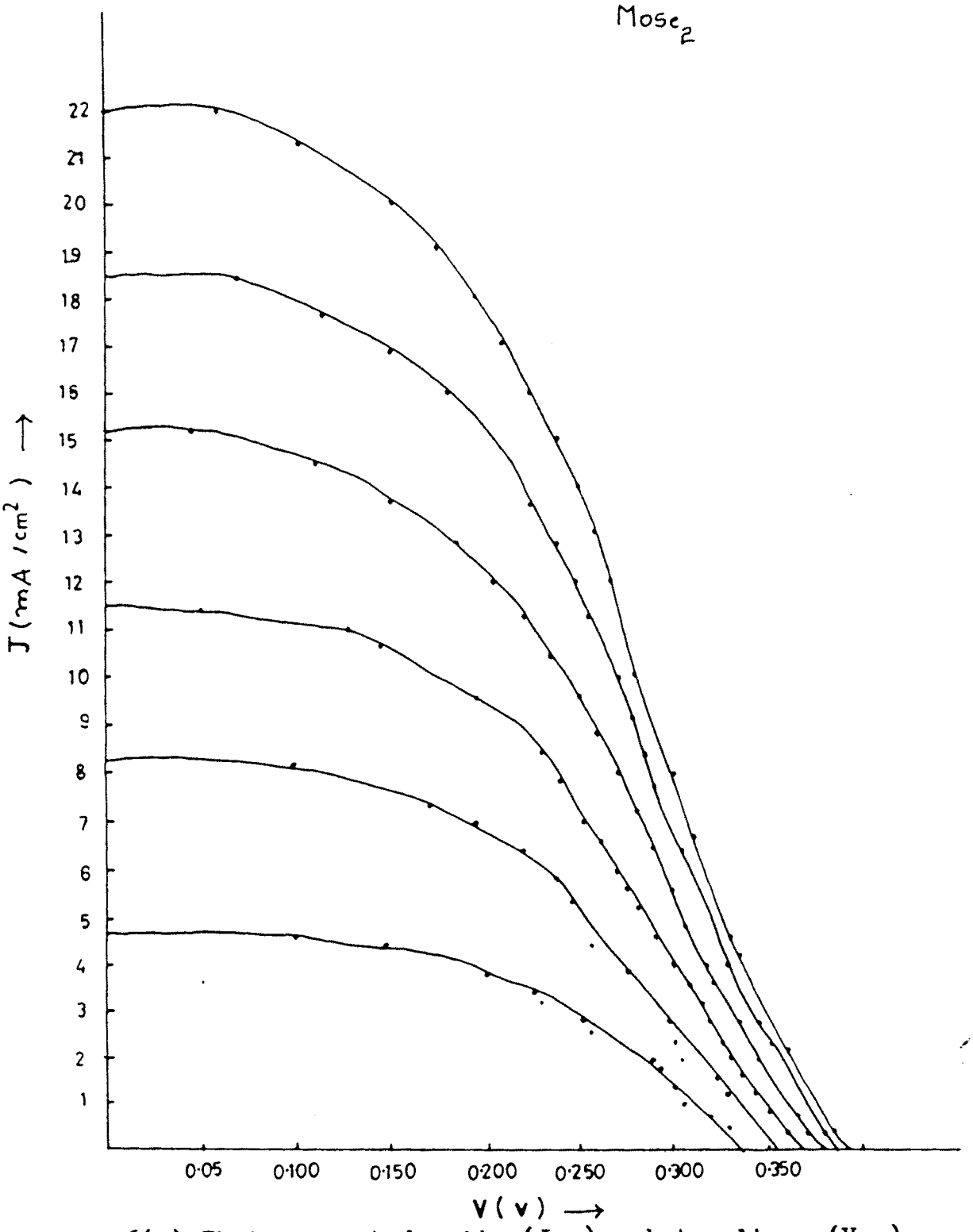


Fig.8.6(a) Photocurrent density ($J_{SC}$), photovoltage ($V_{OC}$) characteristics at different levels of illumination of PEC cell based on $MoSe_2$

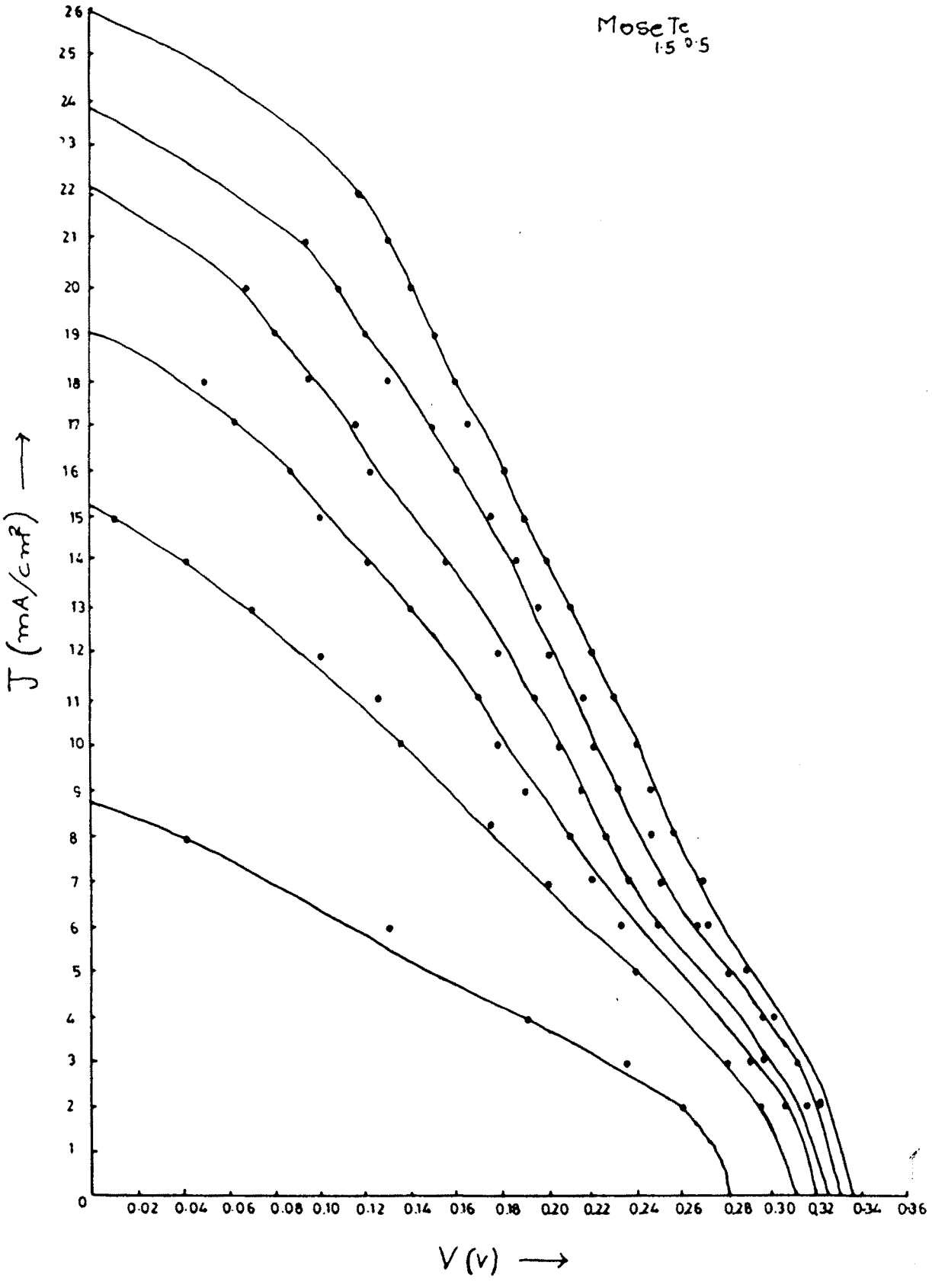


Fig. 8.6(b) Photocurrent density ($J_{SC}$), photovoltage ($V_{OC}$) characteristics at different levels of MoSeT

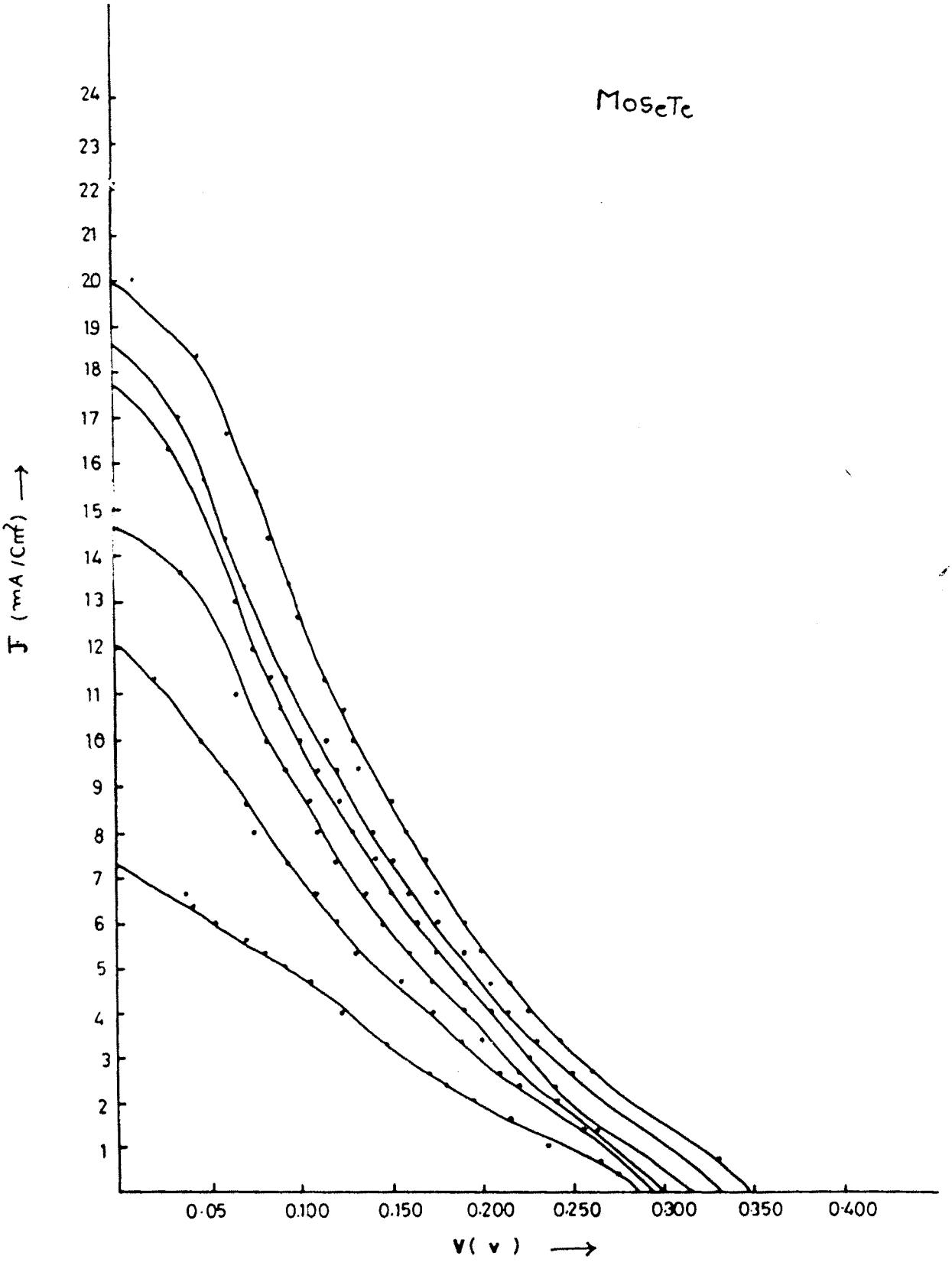


Fig. 8.6(c) Photocurrent density ($J_{SC}$), photovoltage ($V_{OC}$) characteristics at different levels of illumination of PEC cells based on M

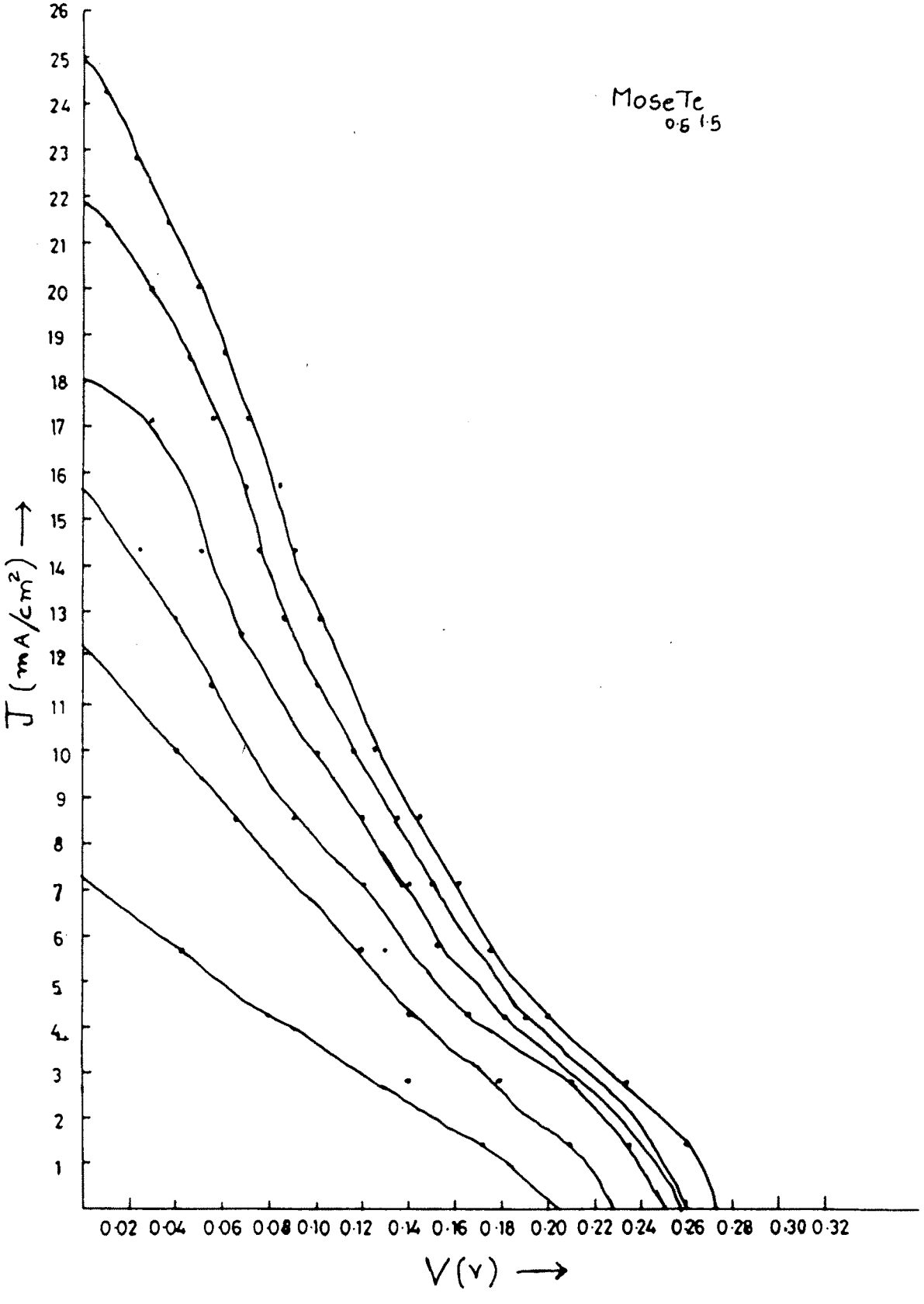


Fig. 8.6(d) Photocurrent density ($J_{SC}$), photovoltage ($V_{OC}$) characteristics at different levels of illuminations of PEC cells based $MoS_{1.5}T$

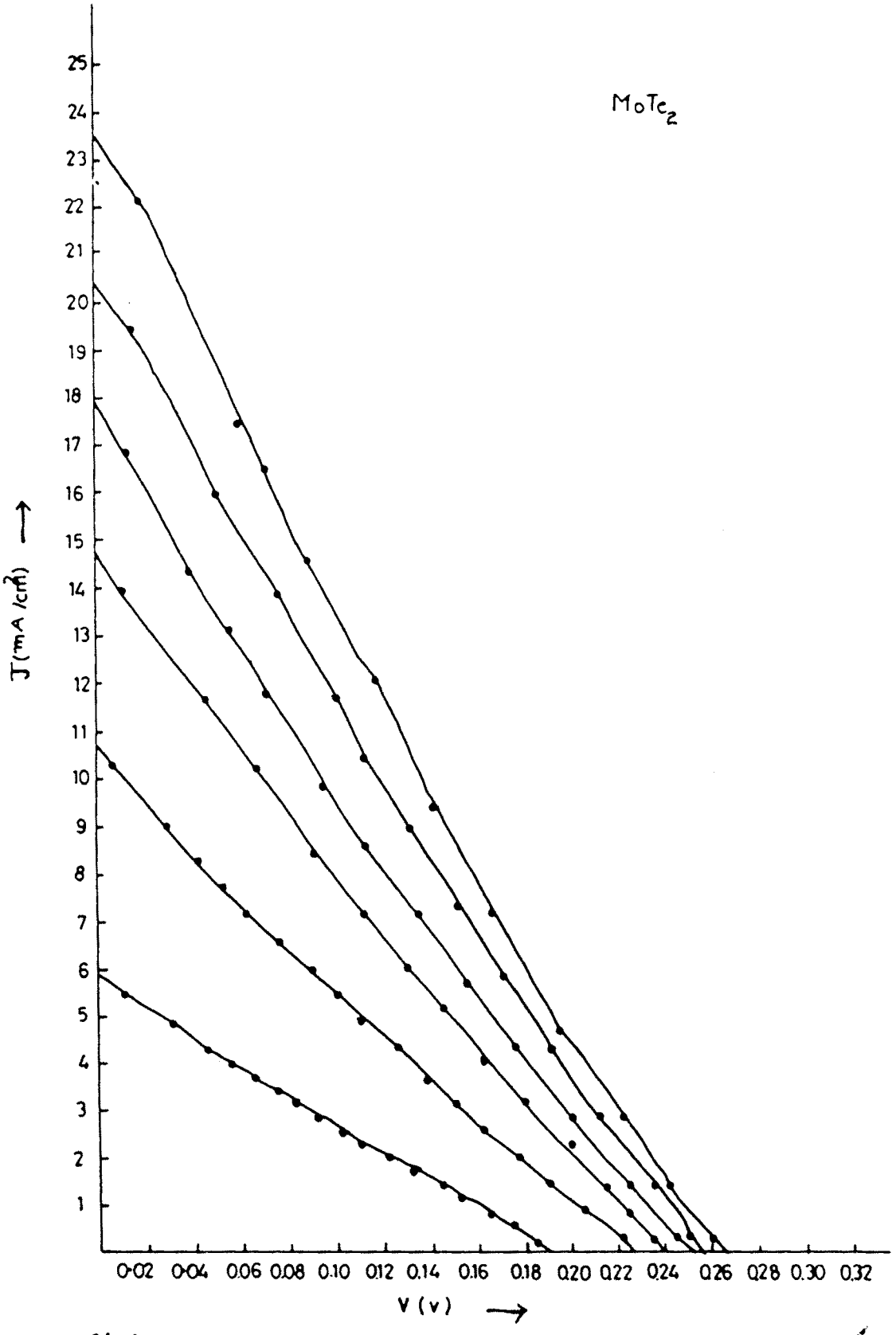


Fig. 8.6(e) Photocurrent density ($J_{SC}$) photovoltage ($V_{OC}$), characteristics at different levels of illumination of PEC cells based on $MoTe_2$

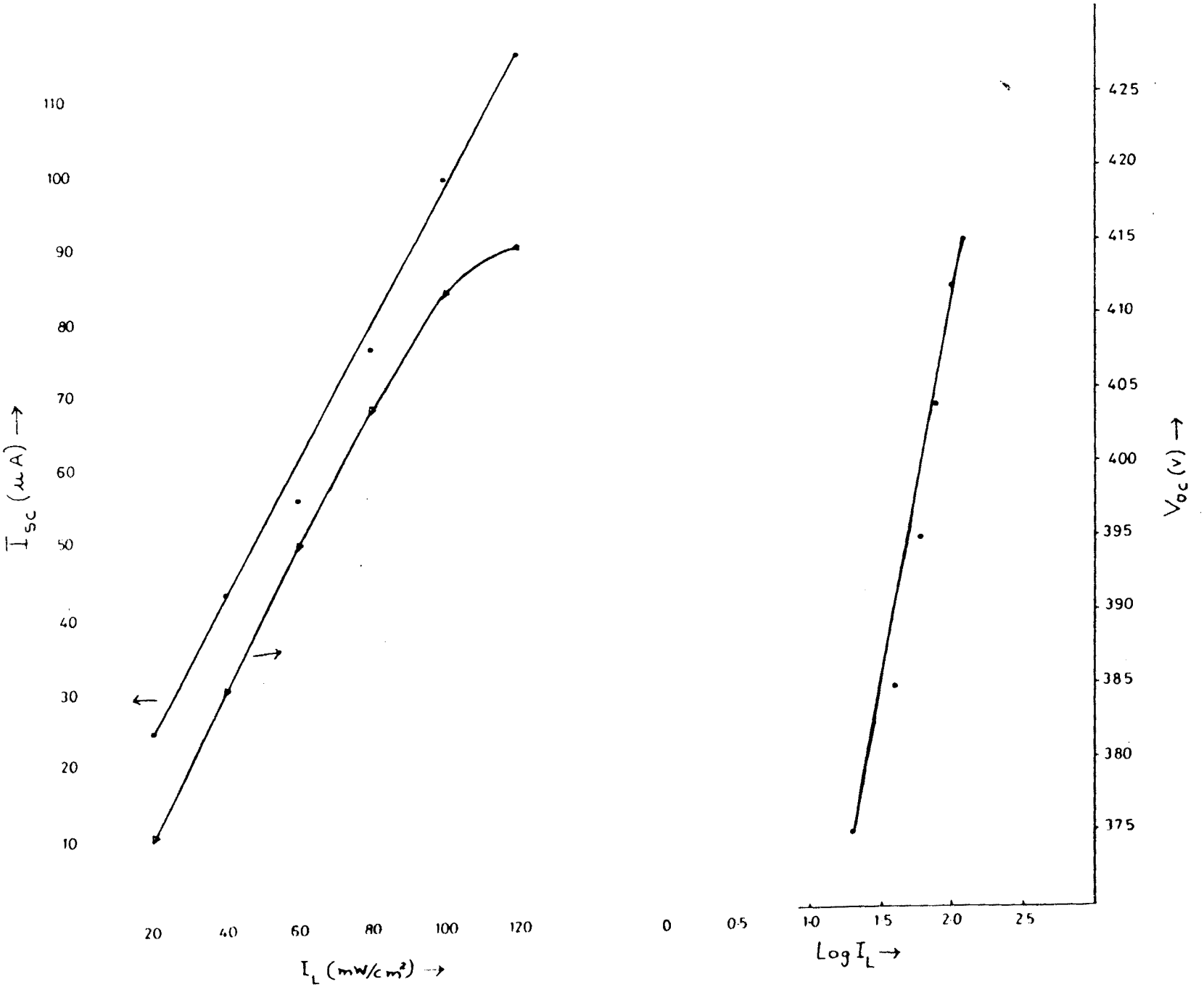


Fig.8.7(a) Plot of $V_{OC}$ and $I_{SC}$ Vs $I_L$ and plot of $V_{OC}$ Vs log $I_L$ for $MoSe_2$

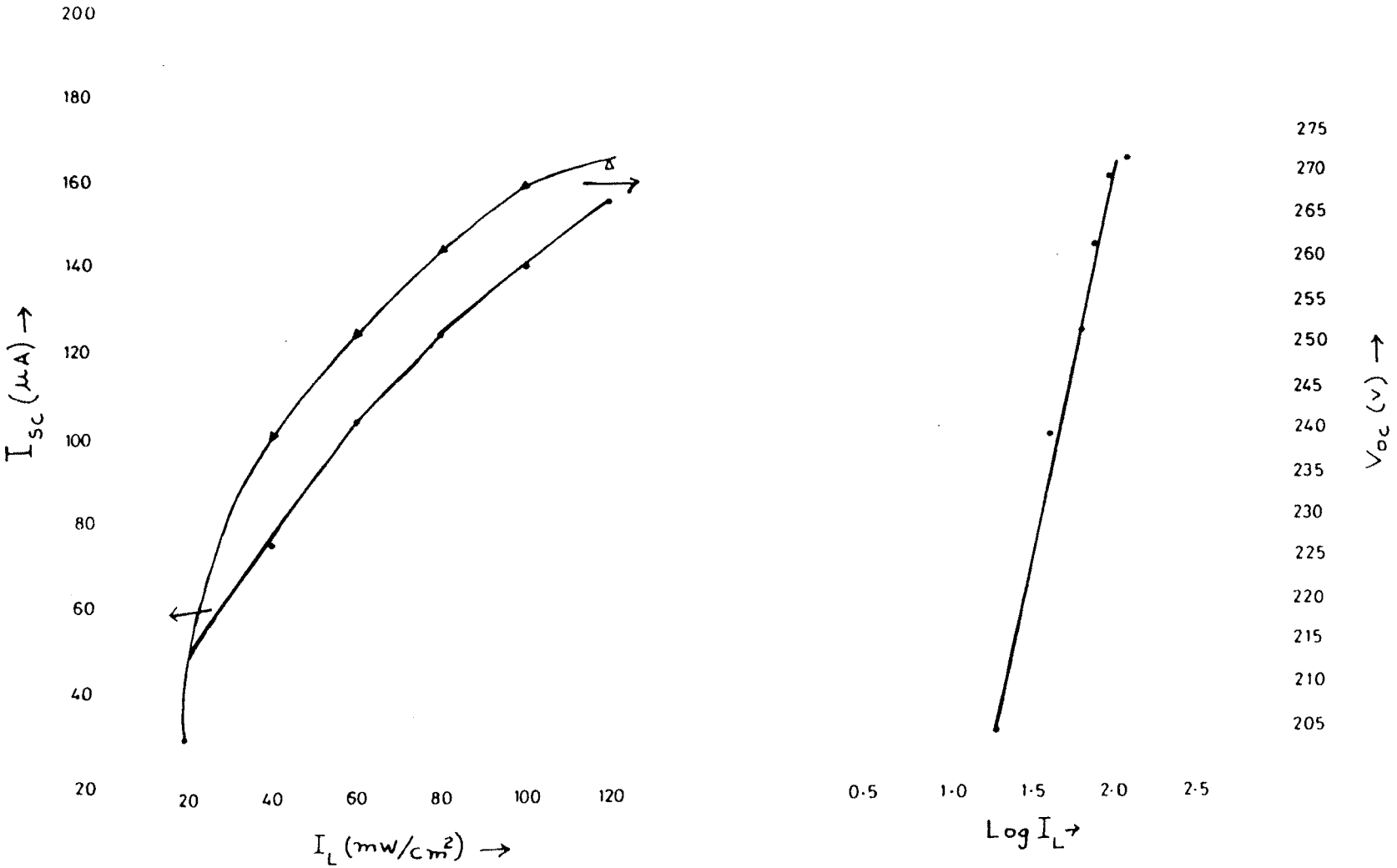


Fig. 8.7(b) Plots of $V_{OC}$ and $I_{SC}$ as a functionof $I_L$ and plots of $V_{OC}$ as a function of log $I_L$ for PEC cell based on $MoSe_{1.5}Te_{0.5}$

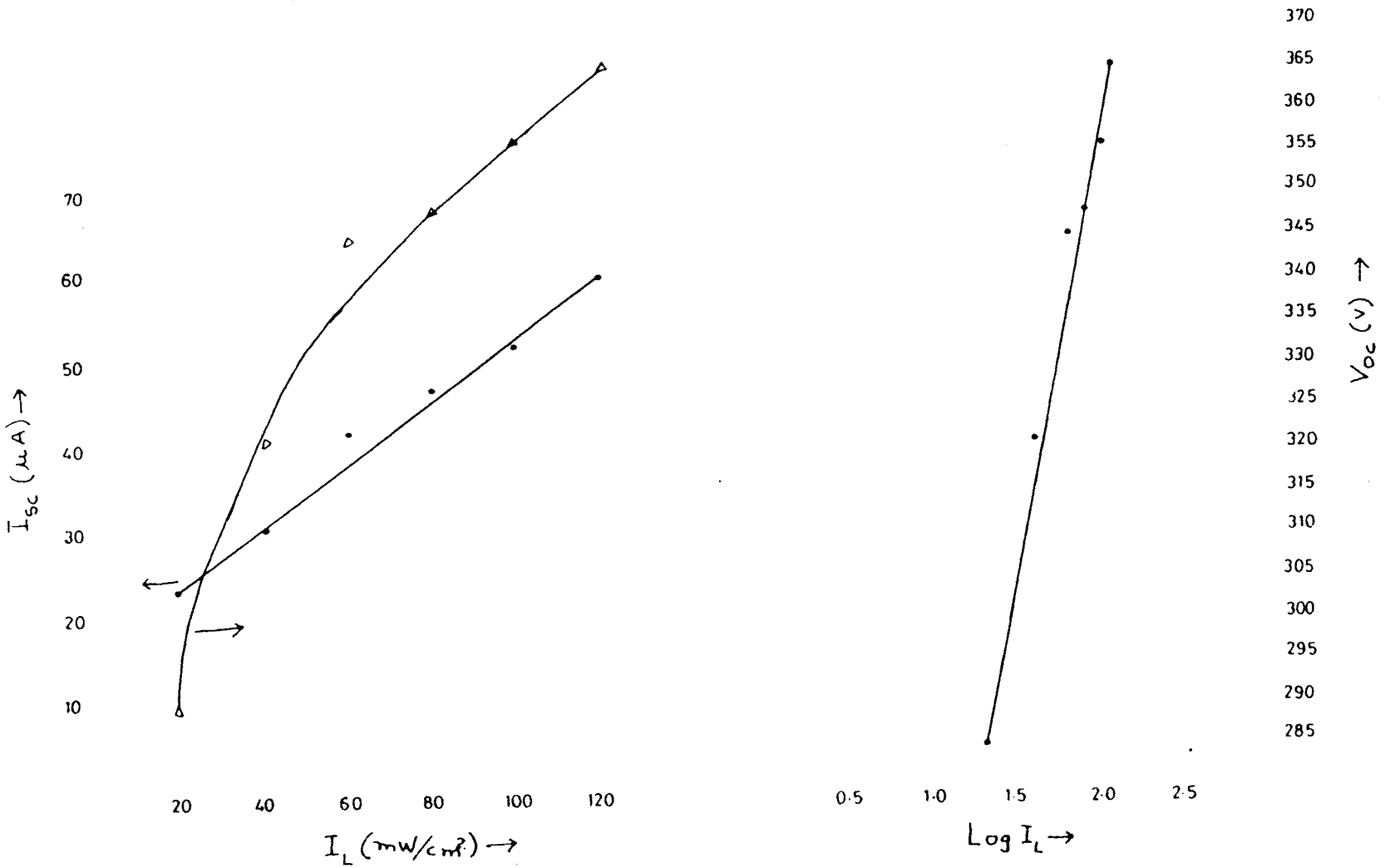


Fig. 8.7(c) Plots of $V_{OC}$ and $I_{SC}$ as a function of light intensity ($I_L$) and plots of $V_{OC}$ as a function of log $I_L$ for PEC cell based on MoSeTe

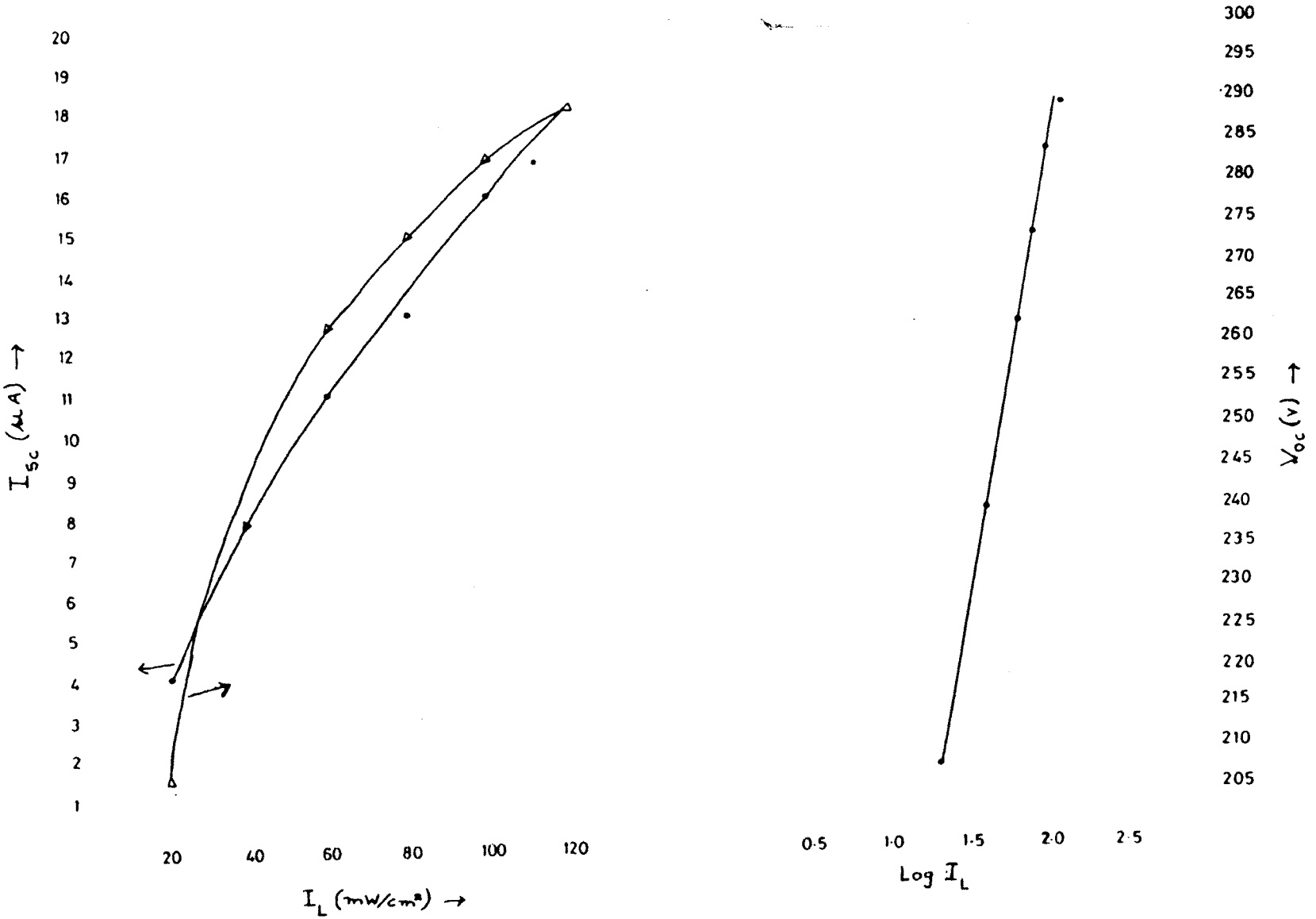


Fig.8.7 (d) Plots of $V_{OC}$ and $I_{SC}$ Vs $I_L$ and plots of $V_{OC}$ Vs log $I_L$ for $MoSe_{0.5}Te_{1.5}$

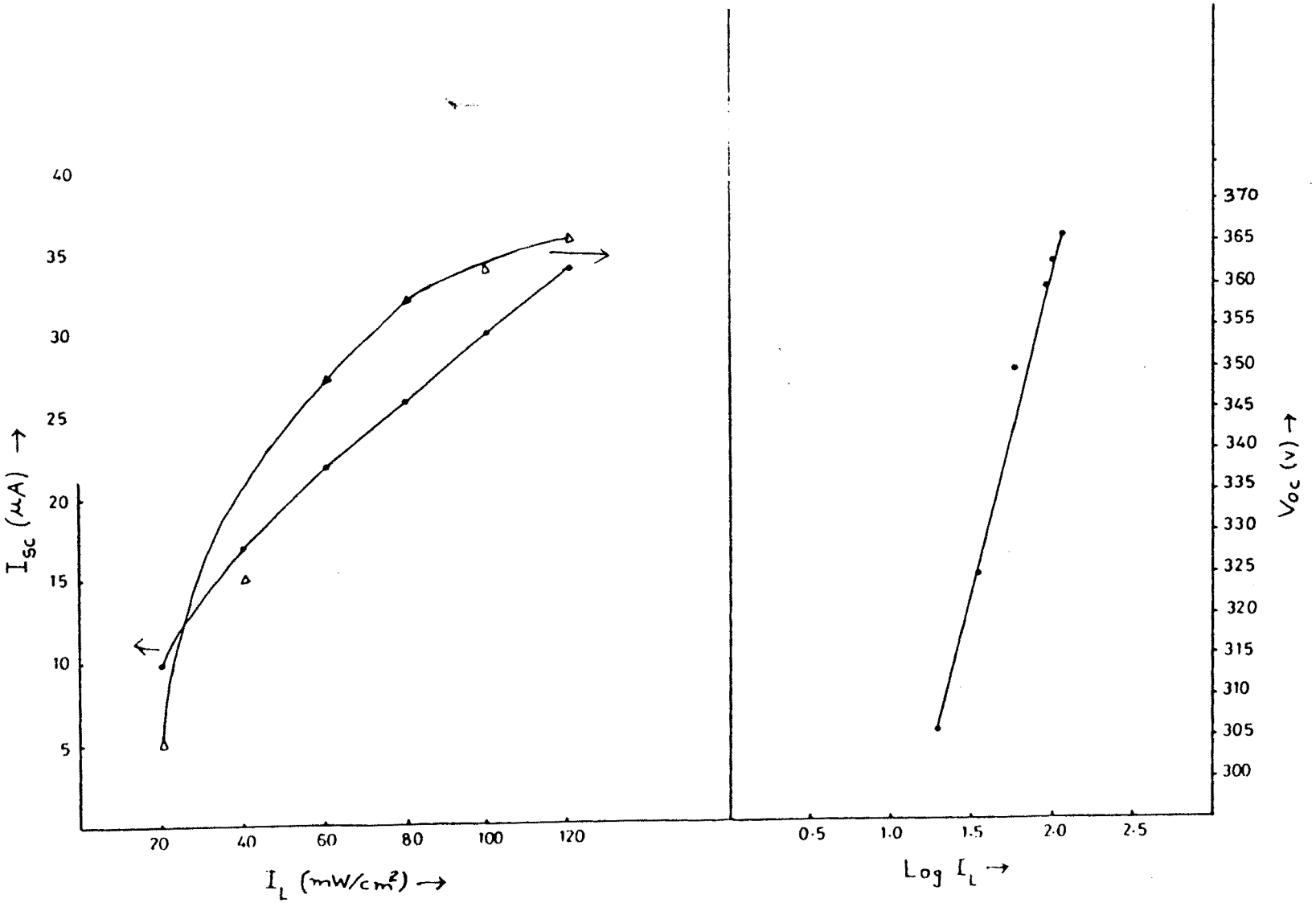


Fig. 8.7(e) Plots of $V_{OC}$ and $I_{SC}$ Vs $I_L$ and plot of $V_{OC}$ Vs log $I_L$ for $MoTe_2$

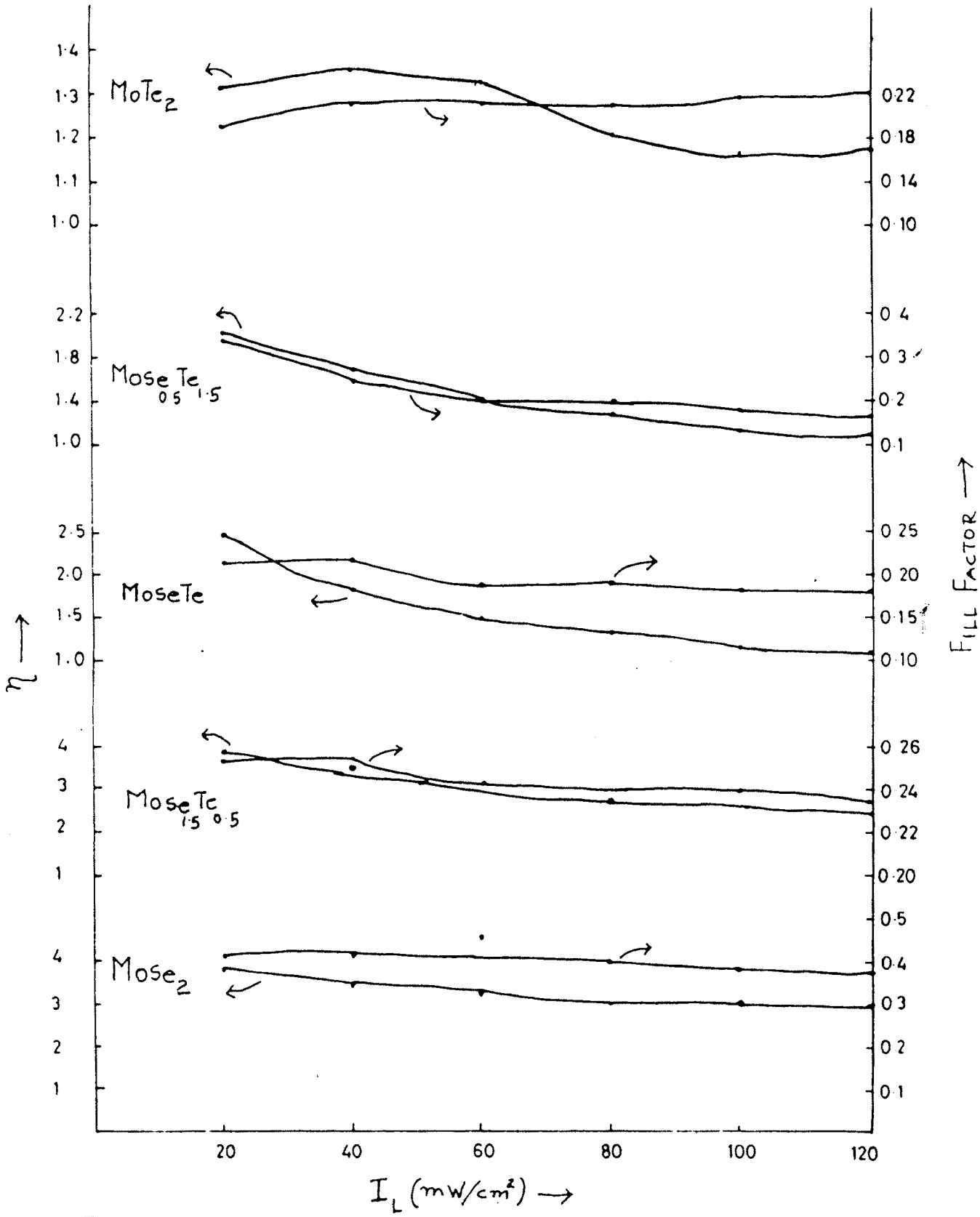


Fig. 8.8 Plots of $\eta$ and Fill factor as a function of $I_L$ for PEC cells based on $MoSe_xTe_{2-x}$ ($0 \leq x \leq 2$)